LA-2185

LOS ALAMOS SCIENTIFIC LABORATORY
OF THE UNIVERSITY OF CALIFORNIA ○ LOS ALAMOS NEW MEXICO

HIGH ENERGY NEUTRONS IN A COLLIMATED BEAM FROM THE LOS ALAMOS FAST PLUTONIUM REACTOR

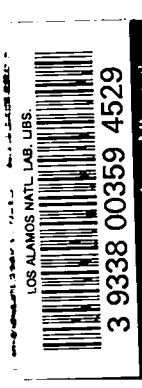

LEGAL NOTICE

LA-2185
PHYSICS AND MATHEMATICS
(TID-4500, 14th edition)

LOS ALAMOS SCIENTIFIC LABORATORY
OF THE UNIVERSITY OF CALIFORNIA LOS ALAMOS NEW MEXICO

REPORT WRITTEN: February 1951

REPORT DISTRIBUTED: February 16, 1959

HIGH ENERGY NEUTRONS IN A COLLIMATED BEAM FROM THE LOS ALAMOS FAST PLUTONIUM REACTOR

by

Bob E. Watt

Contract W-7405-ENG. 36 with the U. S. Atomic Energy Commission

ABSTRACT

Estimates of the excitation energies of fission fragments suggested that it would be useful to search for an upper limit to the neutron energy spectrum. The work reported here was undertaken to extend the fission spectrum as far as was permitted by the beam intensity available from the Los Alamos Fast Plutonium Reactor. A secondary objective was to improve the accuracy of the spectrum reported in Los Alamos Scientific Laboratory Report LA-718. The spectrum reported there was determined from fissions induced by thermal neutrons.

Neutrons were observed in the energy range of 24 to 25 Mev, implying fragment excitation energies greater than 30 Mev. In the spectrum no change of slope is evident, suggesting that fragments of still higher excitation are reasonably abundant.

The objectives of the experiment were: (1) to determine with a precision of 10 per cent or better the number of neutrons emitted from a thick source at 14 Mev relative to the number at some lower energy and (2) to search for an upper limit to fission neutron energies.

Apparatus

A beam of fast neutrons was obtained from the 5W port of the Los Alamos Fast Plutonium Reactor (Clementine)* and allowed to pass through the neutron spectrometer described in Los Alamos Scientific Laboratory Report LA-718 (December 1948).** Figure 1 shows the 5W port and Fig. 2 shows the spectrometer.

Several modifications to the spectrometer were made, primarily to reduce the background count and permit a search for very high energy neutrons in the beam.

Five mil (28.4 mg/cm^2) aluminum absorbers were inserted in the ground planes between counters 1 and 2 and counters 2 and 3 in order to reduce the number of reaction and knock-on particles which could penetrate all three counters. The last absorber also permitted differential counting at the lower energies, resulting in better statistics for a given counting time.

---

*A general description of the reactor has been given by E. J. Jurney et al., Report TID-10048 (LA-1679) (May 1954). Details of the 5W port have been reported by Norris Nereson, Los Alamos Scientific Laboratory Report LA-1234 (February 1951). Nereson used techniques other than the one reported here to study the beam.

**Also B. E. Watt, Phys. Rev. 87, 1037 (1952) (selected data from LA-718).

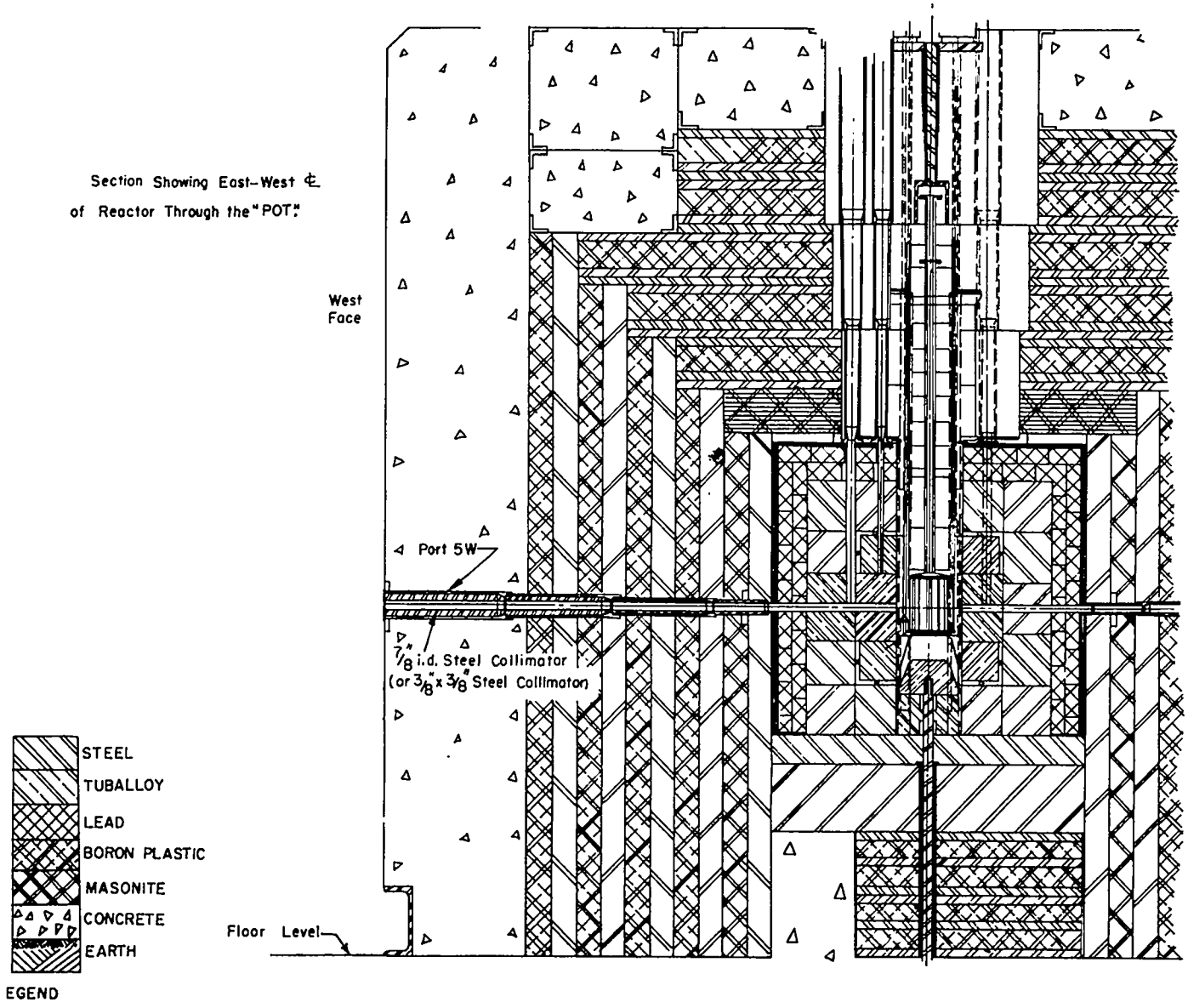

Fig. 1 - The 5W port of the Los Alamos Fast Plutonium Reactor.

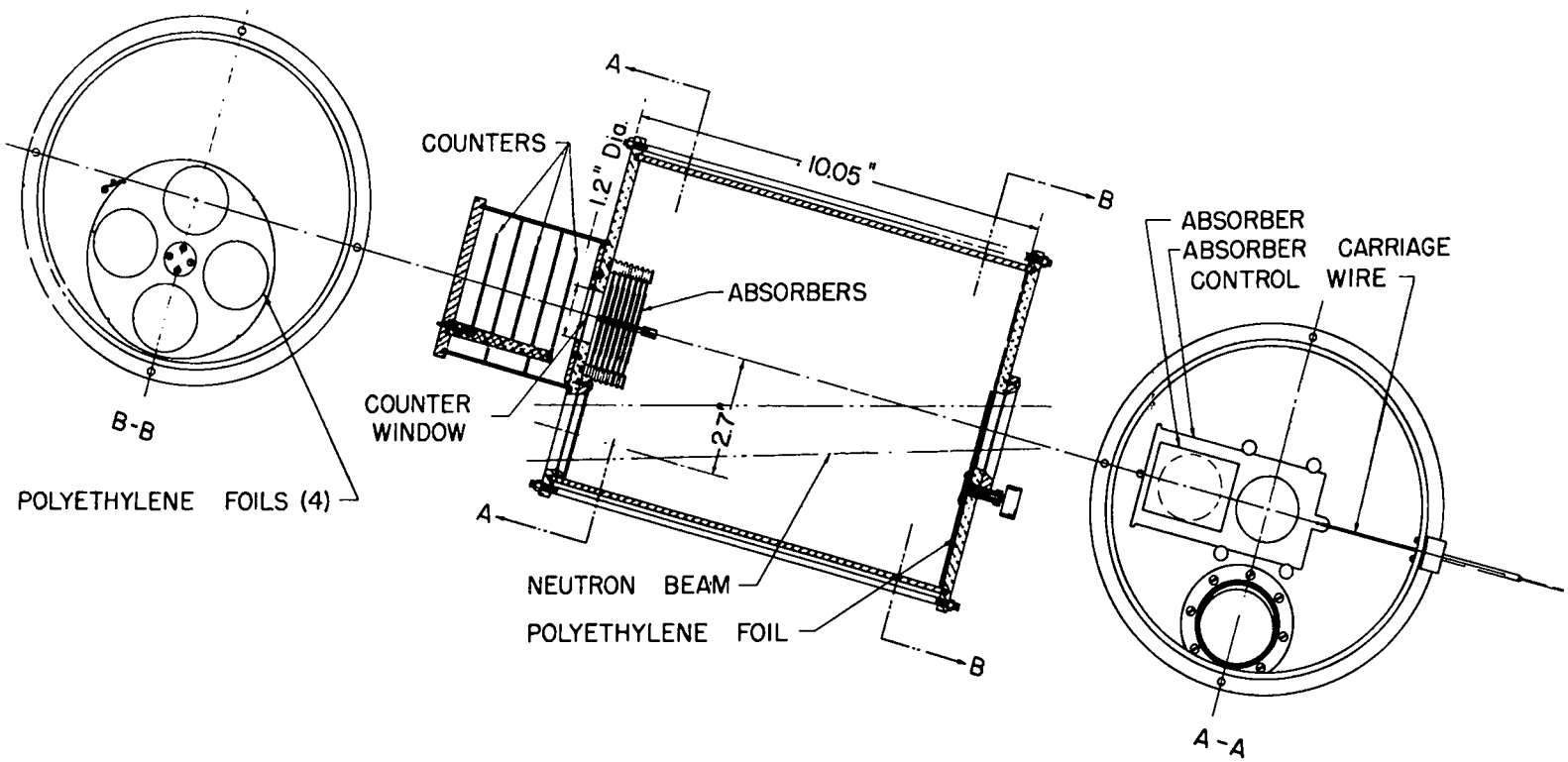

Fig. 2 - Neutron spectrometer. (Figure is from LA-718 and shows the arrangement used with the Los Alamos water boiler region deleted.)

Table I gives the thicknesses of the polythene radiators, and Table II the thicknesses of the various absorbers. The addition of the 5 mil absorbers in the counters required recalculation of the proton energies accepted with particular absorber combinations. The range-energy curves in LA-718 were used and the results are given in Table III. The factor f was obtained from Fig. 12 of LA-718, and ΔE_p was computed using the average rate of energy loss reported by J. H. Smith [Phys. Rev. 71, 32 (1947)]. This was also the source of the range-energy curve.

The equation for neutron flux as related to proton count was derived in LA-718 and is

$$N_n(E) = 5.06 \times 10^4 \frac{\Delta C_p / P(t\rho)}{\sigma_s \Delta E_p} \qquad (1)$$

where $N_n(E)$ is the total neutron flux through the polythene, ΔC_p is the difference in the counts per minute at the two energies for protons, ΔE_p is the proton energy interval in Mev, σ_s the total (np) scattering cross section (isotropy was assumed in the derivation of Eq. 1) in barns, P is the reactor power in kw, and $(t\rho)$ is the thickness of the polythene radiator.

The units of $N_n(E)$ are neutrons/Mev kw sec.

The circuits used were new and permitted rejection of both line pulses and spurious coincidences due to a large pulse in one or more counters. Model 502 amplifiers with a 2 μsec delay line clipping unit were modified slightly to improve the overload characteristics. Three

TABLE I

POLYTHENE RADIATOR THICKNESSES

Polythene Foil	Thickness ($t\rho$), mg/cm^2	Range Equivalent in Aluminum, mg/cm^2
2	2.06	2.88
3	5.70	7.96
4	21.01	29.35
1	71.88	100.4

TABLE II

ALUMINUM ABSORBER THICKNESSES

Absorber	Range Equivalent in Aluminum, mg/cm^2
Counter gas	7.1 ± 1
Counter window	7.42 ± 0.1
Counter absorber	57.0 ± 0.2
1	6.39 ± 0.03
2	13.04 ± 0.05
3	27.0 ± 0.1
4	42.2 ± 0.2
5	110.4 ± 0.4
6	215.8 ± 0.9
7	216.0 ± 2

TABLE III

PROTON ENERGIES

Absorbers		Total Range, mg/cm²					E_p, Mev					E_p(min) + f ΔE_p, Mev					
			Maximum with Radiator					Maximum with Radiator				Radiator					
Number	Thickness, mg/cm²	Min.*	2	3	4	1	Min.	2	3	4	1	2	3	4	1	ΔR, mg/cm²	ΔE_p, Mev
0	0	71.5	74.4	79.5	100.9	171.9	6.12	6.28	6.50	7.53	10.18	6.2	6.30	6.74	7.52		
2	13.04	84.1		92.05	113.44		6.72		7.09	8.05			6.87	7.32		13.04	0.62
3	27.00	98.5		106.46	127.85		7.38		7.75	8.59			7.56	7.92		13.96	0.63
4	42.2	113.7		121.7	143.0		8.02		8.36	9.16			8.19	8.53		15.2	0.643
3,4	69.20	140.7		148.7	170.0		9.08		9.36	10.14			9.22	9.57		27.00	1.05
1-4	88.2	159.76		167.6	189.0	260.1	9.80		10.07	10.76	12.92		9.93	10.24	11.0	19.4	0.695
2,5	123.4	194.9		202.8	224.2	295.3	10.96		11.16	11.9	13.9		11.06	11.40	12.08	35.2	1.17
1,4,5	158.9	230.4		238.4	259.8	230.8	12.06			12.9	14.8			12.45	13.1	35.5	1.10
2-5	192.6	264.1			293.4	364.5	13.03			13.82	15.64			13.43	14.1	33.7	0.974
2,6	228.8	300.3			329.7	400.7	14.00			14.78	16.48			14.36	14.99	36.2	0.988
2,4,6	271.0	342.5			371.9	442.9	15.08			15.80	17.46			15.41	16.03	42.2	1.09
1-4,6	304.4	375.9				476.3	15.92				18.20				16.85	33.4	0.818
3,5,6	353.2	424.6				525.0	17.06				19.24				17.95	48.8	1.14
3-6	395.3	466.8				567.2	17.99				20.08				18.87	42.2	0.937
2,6,7	444.6	516.1				616.5	19.05				21.03				19.88	49.3	1.05
2,4,6,7	486.8	558.3				658.7	19.90				21.86				20.72	42.2	0.865
5-7	542.0	613.4				713.8	21.00				22.86				21.78	55.2	1.09
4,5-7,2	597.2	668.6				769.0	22.04				23.84				22.81	57.2	1.09
1-7	630.6	702.1				802.5	22.64				24.42				23.40	33.4	0.615

*With air at 22 inches Hg.

were connected to the counters and a fourth was connected to a dummy chamber (a capacitance), which was connected to the spectrometer. Line pulses were effectively canceled with this setup.

The counter construction was such that a small coupling capacitance existed between all counters, with the result that a specific counter would register a spurious pulse if a pulse 70 times larger than the detection threshold occurred in another counter. Spurious coincidences from this source were avoided by using the coincidence circuit described in LASL drawing 4Y-26121 and by operating in "channel" coincidence.

The dual output, five input unit described in the drawing permits independent selection of the operation of all inputs, and two independent coincidence circuits are operated from the same inputs to permit simultaneous observations with either the same or different input combinations.

Each input can be:

1. Disconnected.
2. Operated in coincidence. A pulse larger than the common detection threshold is required for an output pulse.
3. Operated in channel. A pulse larger than the common detection threshold but smaller than the individually set anticoincidence level is required for an output pulse.
4. Operated in anticoincidence. Any pulse larger than the individually set anticoincidence level will prevent an output pulse.

The Model 502 amplifiers could deliver 33 to 35 volt pulses at the 100 line terminations in the coincidence circuit, and the lowest detection level desirable was 2 volts. The maximum useful channel width for

any particular input was then 15:1, which was used for counters 1 and 2. The acceptable range of pulse heights from counter 3 had to be considerably larger than the range from 1 and 2 because the proton might stop in the chamber or might pass through with considerable energy. In addition, all pulses were not amplified the same amount in the gas, resulting in a pulse height spread of about 30:1 from counter 3. To provide channel operation with a ratio of 40:1, it was necessary to connect a fifth amplifier to the output of the preamplifier for counter 3 and operate it in anticoincidence.

It was observed that the pulses from counter 2 were about 25 per cent larger than those from counter 1, in part due to the protons' greater specific ionization. The gains were set to give about equal output pulses and a detection level in the coincidence circuit corresponding to about 0.1 mv from the counters. The gain for counter 3 was set to be the same as for counter 1, as no direct evidence of pulse heights for relatively high energy protons was available.

Table IV shows the output voltage from each of the three counters which was required for a coincidence or which would prevent an output by anticoincidence.

TABLE IV

COUNTER PULSE HEIGHTS

Counter	Output Voltage for Coincidence, mv	Output Voltage for Anticoincidence, mv	Channel Width
1	0.09	1.3	15:1
2	0.11	1.7	15:1
3	0.09	3.6	40:1

With the settings used, any pulse large enough to give a coincidence by capacity coupling to the other counters was also above its own anti-coincidence level.

With the operating voltages on the counters, but no beam, the background rate was less than 0.01 cpm. With the full power beam through the apparatus the lowest counting rate reached was 0.03 cpm, at least 50 per cent of which is believed to be due to protons capable of penetrating all the absorbers available.

Counter Characteristics

As a guide in estimating the gas amplification and channel widths necessary, the energy loss in each of the three channels was computed for a 6 Mev proton and a 12 Mev proton leaving the inside of the 1 mil window. The values computed are given in Table V.

TABLE V

ENERGY LOSS IN THE CHANNELS

Proton Energy, Mev	Energy Loss, Mev		
	Counter 1	Counter 2	Counter 3
6	0.14	0.2	0.85
12	0.085	0.09	

For the input circuit used

$$AE/V = 8$$

where

A = gas amplification

E = the ionization energy loss in Mev

V = pulse voltage output in mv

As it proved convenient to set the detection level at about 0.1 mv, AE = 0.8 Mev. As shown in Table V, the minimum gas amplification had to be at least 10 to observe the more energetic protons and so get a reasonably accurate integral count.

From the relation

$$R = 4.16 \times 10^{-3} E^{1.73} \qquad (2)$$

it is computed that an electron capable of penetrating all three counters (R = 64 mg/cm^2 = 43 cm of air) has an energy loss rate

$$\frac{dE}{dR} = 23.6\ R^{-0.42} = \frac{23.6}{4.8} = 4.9 \text{ kev/cm} \qquad (3)$$

For 6 Mev protons

$$\frac{dE}{dR} = 77 \text{ kev/cm}$$

which is 16 times the calculated rate for the electrons.

From the curves for counting rate vs voltage, Fig. 3, and the pulse height distribution at the electron count threshold (1.9 kv), Fig. 4, it seems that the ratio of maximum proton pulse height to maximum electron pulse height (threshold) is more nearly 7.5:1 than the 16:1 expected. This is regarded as acceptable agreement in view of the errors associated with Eq. 2 and the possibility of longer electron paths in at least the first counter.

The maximum energy loss by the electrons is then observed to be about 19 kev, and the energy lost by a 12 Mev proton is 85 kev, only 4.5 times the value for the electrons. The pulse height distribution seems to imply a rather large spread (of the order 5:1) for a given energy loss, which results in less than unity efficiency for the counters.

The efficiency of counter 2 was checked at several voltages by comparing 1, 3 coincidences with 1, 2, 3 coincidences and was found to be 97 per cent efficient for the protons giving a 1, 3 coincidence. Because amplifier gains of counters 1 and 2 were set to deliver the same range of pulse heights, counter 1 is expected to have the same efficiency as counter 2. Unfortunately, a direct comparison of 1, 2, 3 coincidences with 2, 3 coincidences can only set a lower bound, observed

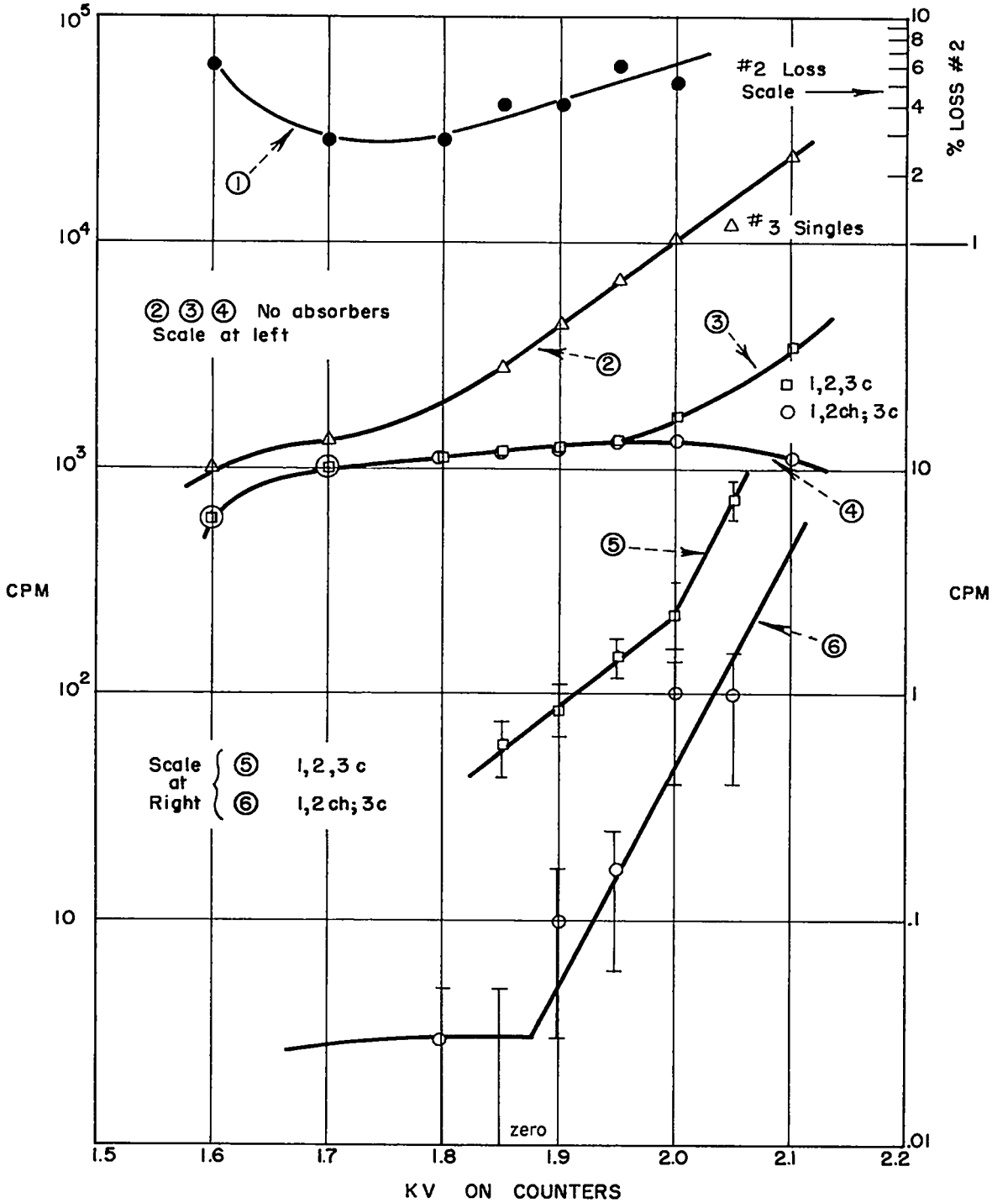

Fig. 3 - Counting rate vs counter voltage.

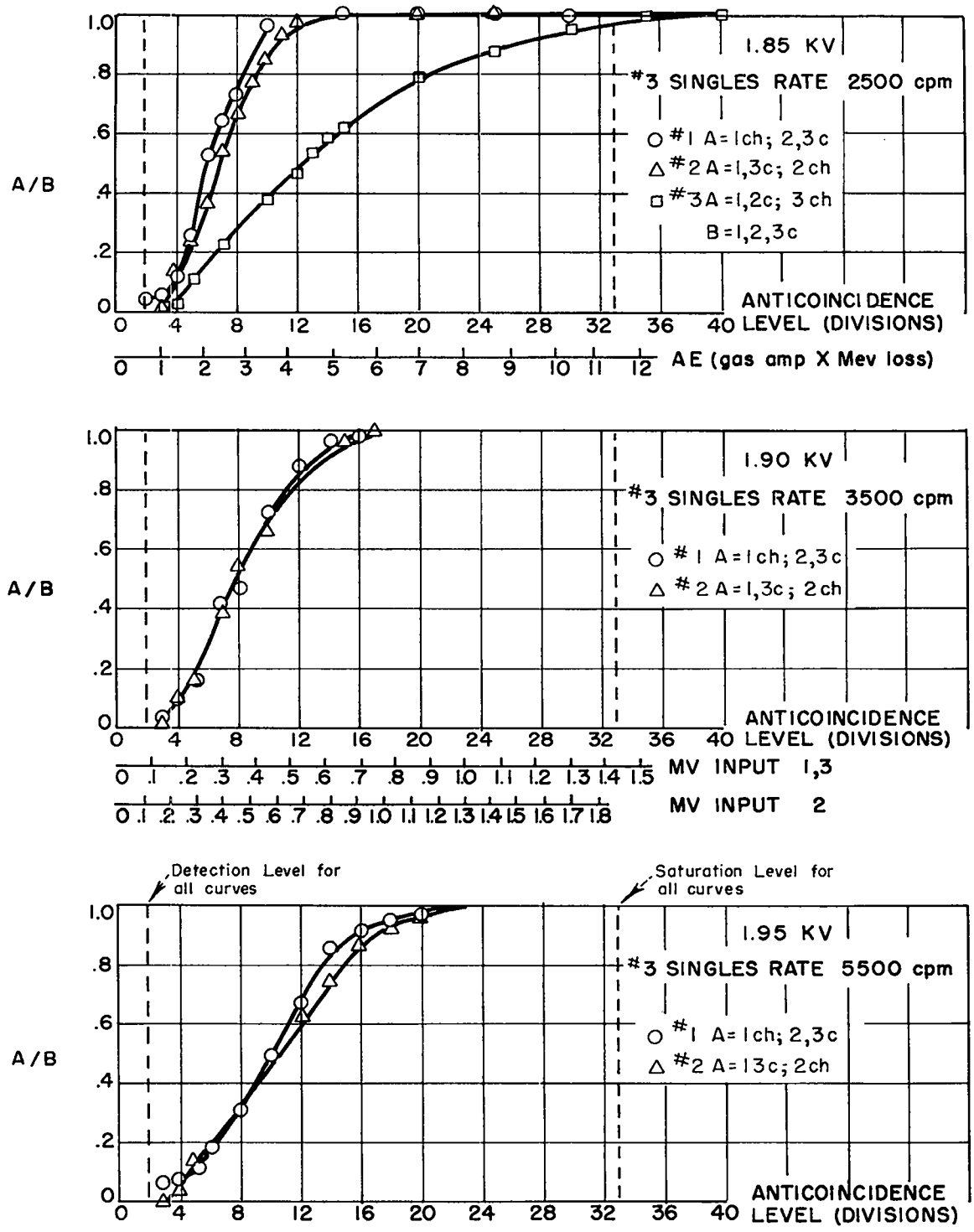

Fig. 4 - Pulse height distribution.

to be 90 per cent, owing to the uncertainty that the 2, 3 coincidence was caused by a proton which traversed counter 1. Since the energy distribution of the protons penetrating the counters is nearly independent of the preceding absorber combination, it is thought that all such efficiency factors appear only in the constant determining the absolute neutron flux, leaving the relative accuracy of various points untouched.

The intensity computed for the integral and differential methods will, however, be different if the 1, 2, 3 coincidence efficiency is different from the 1, 2 coincidence efficiency.

The counting efficiency is a function of both the spatial distribution and energy of the protons. The spatial distribution is independent of the absorber combinations preceding the counters, so define $f_i(E_c)$ as the space averaged counting efficiency, a function only of the proton energy on entering the counters (E_c).

Assume that the proton distribution is exponential in the range of interest, because assumptions nearer to the conditions of this experiment lead to series expressions for the integrals. The proton count can then be written

$$C_{pi} = K \int_0^\infty f\,(E - E_{Li})\, e^{-E/Q}\, dE$$

where E_{Li} is the energy lost by a proton of initial energy E in the absorber combination preceding the counters. It is also a function of E, but a relatively slow one, being given reasonably well by the relation

$$E_{Li} \cong {}_oE_{Li} - k(E - {}_oE_{Li} - E_o)$$

where ${}_oE_{Li}$ is the loss by a proton entering the counters with the minimum detection energy E_o, and k is a constant depending on the value of $(E_o + {}_oE_{Li})$: $k = 0.08$ for $(E_o + {}_oE_{Li}) = 6$ Mev and $k = 0.04$ for $(E_o + {}_oE_{Li}) = 12$ Mev.

$$C_{pi} = K \int_o^\infty f\left[(1 + k_i)\ (E - {}_oE_{Li}) - k_i E_o\right] e^{-E/Q}\, dE$$

Defining $\bar{f}_i$ by the ratio

$$\bar{f}_i = \frac{K \int_{(E_o + {}_oE_{Li})}^\infty f\left[(1 + k_i)\ (E - {}_oE_{Li} - k_i E_o\right] e^{-E/Q}\, dE}{K \int_{(E_o + {}_oE_{Li})}^\infty e^{-E/Q}\, dE}$$

we expect $\bar{f}_i$ to vary only very slowly with various absorber combinations $({}_oE_{Li})$, as k_i is small and varies slowly. If f rises to a constant value in a small energy interval, the variation with energy is unimportant.

Then

$$C_{pi} = K \bar{f}_i \int_{(E_o + {}_oE_{Li})}^\infty e^{-E/Q}$$

$$= K \bar{f}_i\ Q\ e^{-(E_o + {}_oE_{Li})/Q}$$

The difference between two integral counts is then

$$\Delta C_{pab} = KQ\left[\bar{f}_a\, e^{-(E_o + {}_oE_{La})/Q} - \bar{f}_b\, e^{-(E_o + {}_oE_{Lb})/Q}\right]$$

$$= KQ\,\bar{f}\left[e^{-(E_o + {}_oE_{La})/Q} - e^{-(E_o + {}_oE_{Lb})/Q}\right]$$

if $\bar{f}_a = \bar{f}_b$.

Let $\bar{f}_2$ be the average efficiency for 1, 2 coincidence, $\bar{f}_3$ the average efficiency for 1, 2, 3 coincidence, and write the energies $(E_o + E_{Li})$ as E_i.

Then

$$\Delta C_p(\text{integral}) = KQ\left[e^{-E_1/Q} - e^{-E_2/Q}\right]\bar{f}_3$$

and

$$\Delta C_p(\text{differential}) = KQ\left[\bar{f}_2\, e^{-E_1/Q} - \bar{f}_3\, e^{-E_2/Q}\right]$$

Then

$$\frac{\Delta C_p(\text{differential})}{\Delta C_p(\text{integral})} = 1.4 = \frac{\bar{f}_2\, e^{-E_1/Q} - \bar{f}_3\, e^{-E_2/Q}}{\bar{f}_3\left[e^{-E_1/Q} - e^{-E_2/Q}\right]}$$

$$1.4\,\bar{f}_3\left[e^{-E_1/Q} - e^{-E_2/Q}\right] + \bar{f}_3\, e^{-E_2/Q} = \bar{f}_2\, e^{-E_1/Q}$$

$$\bar{f}_2 = 1.4\left[1 - e^{-(E_2 - E_1)/Q}\right] + e^{-(E_2 - E_1)/Q}$$

$$\bar{f}_3 = 1.4 - 0.4\, e^{-(E_2 - E_1)/Q}$$

For $(E_2 - E_1) = 1$ Mev and $Q = 1.4$ Mev, we have $\bar{f}_2/\bar{f}_3 = 1.2$, or $\bar{f}_3/\bar{f}_2 = 0.83$. The ratio $\bar{f}_2/\bar{f}_3$ is surprisingly large. However, the relative intensity at various energies is thought to be correct within the statistical errors.

The observations, with the calculations of N(E), are presented in Tables VI through XI.

Unfortunately, it was necessary to take the data over a rather extended time, during which the power monitoring systems on the reactor showed signs of drift. The power obtained by a heat balance was thought to be the most reliable so it was entered in the power column. The data in Tables X and XI were taken in a single day and hence are thought to be the best for determining relative intensities. None of the runs indicated deviations from a smooth curve which is nearly a straight line on a semi-log plot.

Figure 5 is a plot of all the data, except the differential method, with the photographic plate data obtained by Norris Nereson.* Figure 6 is a plot of selected data from the present experiment.

---

*See Report LA-1234.

TABLE VI

EXPERIMENTAL DATA

P, kw	Radiator No.	Absrs.	Counts A	Counts B	Counts C	t, min	Counts per Minute A	Counts per Minute B	Counts per Minute C	$C_p/P(t\rho)$, protons / kw mg/cm^2	E_{pl}, Mev	ΔE_p, Mev	$E_{pl} + f\Delta E_p$, Mev	E_n, Mev	σ_s, barns	$\Delta[C_p/P(t\rho)]$, counts / kw min mg/cm^2	N(E) x 10^{-4}, neutrons / Mev kw sec
22.6	3	0	1582	1548	3658	5	316 ± 8	310 ± 8	732 ± 12	2.45 ± 0.06	6.30	0.62	6.60	7.1	1.30	0.97 ± 0.08	6.10 ± 0.5
22.6	3	2	1150	1124	3778	6	192 ± 6	187 ± 6	640 ± 10	1.48 ± 0.05	6.87	0.63	7.17	7.70	1.17	0.545 ± 0.06	3.75 ± 0.4
22.6	3	3	1090	1074	4916	9	121 ± 4	120 ± 4	536 ± 8	0.93 ± 0.03	7.56	0.64	7.86	8.45	1.08	0.443 ± 0.04	3.25 ± 0.3
22.6	3	4	1036	1014	7918	16	64.7 ± 2	63.4 ± 2	495 ± 6	0.49 ± 0.015	8.19	1.05	8.67	9.33	1.00	0.272 ± 0.016	1.32 ± 0.08
22.6	3	3,4	970	958	14168	34	28.5 ± 0.9	28.2 ± 0.9	416 ± 3.5	0.22 ± 0.007	9.22	0.69	9.55	10.27	0.93	0.094 ± 0.008	0.737 ± 0.07
22.6	3	1-4	492	486	11376	30	16.4 ± 0.7	16.2 ± 0.7	378 ± 3	0.12 ± 0.005	9.93	1.17	10.46	11.24			
0	3	1-7	0	2	1598	92	0	0.02	17.4								
22.6	3	0	1558	1538	3376	5	312 ± 8	308 ± 8	675 ± 12	2.42 ± 0.06							
22.6	4	0	1462	1428	2148	2	731 ± 19	714 ± 19	1074 ± 23	1.54 ± 0.04							
22.6	4	3,4	1012	998	~7000	15	67.5 ± 2	66.5 ± 2	470	0.142 ± 0.004	9.57	0.695	9.90	10.64	0.89	0.052 ± 0.004	0.43 ± 0.04
22.6	4	1-4	1032	1004	10128	24	43.0 ± 1	41.8 ± 1	422 ± 4	0.090 ± 0.002	10.24	1.17	10.77	11.58	0.82	0.059 ± 0.002	0.30 ± 0.01
22.6	4	2,5	1006	1000	29004	68	14.8 ± 0.5	14.7 ± 0.5	426 ± 2.5	0.031 ± 0.001	11.40	1.10	11.90	12.80	0.75	0.016 ± 0.001	0.098 ± 0.008
22.6	4	1,4,5	176	176	9426	24	7.3 ± 0.6	7.3 ± 0.6	385 ± 4	0.015 ± 0.001							

TABLE VII

EXPERIMENTAL DATA

P, kw	Radiator No.	Absrs.	Counts A	Counts B	Counts C	t, min	Counts per Minute A	Counts per Minute B	Counts per Minute C	$C_p/P(t\rho)$, protons / kw mg/cm^2	E_{pl}, Mev	ΔE_p, Mev	$E_{pl} + f\Delta E_p$, Mev	E_n, Mev	σ_s, barns	$\Delta[C_p/P(t\rho)]$, counts / kw min mg/cm^2	$N(E) \times 10^{-2}$, neutrons / Mev kw sec
24.3	4	2,5	1122	1128	87356	61	18.4 ± 0.5	18.5 ± 0.5	1432	$(3.61 \pm 0.1) \times 10^{-2}$	11.4	1.10	11.90	12.80	0.75	$(2.16 \pm 0.11) \times 10^{-2}$	13.3 ± 0.7
24.3	4	1,4,5	636	638	118654	88	7.25	7.25	1350								
24.3	4	1-7	0	0	4384	74	0	0	59.3								
24.3	4	1,4,5	372	372	60048	48											
Sum of runs			1008	1010		136	7.41 ± 0.23	7.43 ± 0.23		$(1.45 \pm 0.05) \times 10^{-2}$	12.45	0.97	12.90	13.90	0.69	$(7.6 \pm 0.6) \times 10^{-3}$	5.76 ± 0.4
24.0	4	2-5	508	510	163972	141	3.6 ± 0.16	3.62 ± 0.16	1160								
0	4	2-5	0	0	9422	151	0	0									
Sum	4	2-5	564	566		161	3.50 ± 0.15	3.52 ± 0.15		$(6.9 \pm 0.3) \times 10^{-3}$	13.43	0.98	13.88	14.92	0.64	$(4.0 \pm 0.35) \times 10^{-3}$	3.2 ± 0.3
	4	2-5	56	56	21034	20	2.8 ± 0.4		1050								
	4	2,6	12	12	10052	10	1.2	1.2	1005								
23.7	1	0	1240	1242	2514	1		1.9 kv									
23.7	1	0	1276	1284	3678	1		1.95 kv									
23.7	1	0	1306	1308	5450	1		2.0 kv									
23.7	4	2,6	152	150	208824	103	1.47 ± 0.12	1.45 ± 0.12	2030	$(2.9 \pm 0.2) \times 10^{-3}$	14.4		14.9	16.0	0.59	$(2.9 \pm 0.2) \times 10^{-3}$	1.5 ± 0.1
0	4	2,6	0	0	862	17	0	0									
2	1	0	1290	1296	3436	1											

TABLE VIII

EXPERIMENTAL DATA

P, kw	Radiator No.	Absrs.	Counts A	Counts B	Counts C	t, min	Counts per Minute A	Counts per Minute B	Counts per Minute C	$C_p/P(t\rho)$, protons / kw mg/cm^2	E_{p1}, Mev	ΔE_p, Mev	$E_{p1} + f\Delta E_p$, Mev	E_n, Mev	σ_s, barns	$\Delta[C_p/P(t\rho)]$, counts / kw min mg/cm^2	N(E), neutrons / Mev kw sec
23.2	1	0	1290	1296	3436	1											
23.2	1	1,4,5	1072	1072	148602	82	13.1 ± 0.4	13.1 ± 0.4	1810	(7.85 ± 0.36) x 10^{-3}	13.1	0.97	13.55	14.6	0.65	(4.05 ± 0.4) x 10^{-3}	325 ± 30
23.2	1	2-5	574	572	158912	91			1750								
23.2	1	2-5	0	0	4260	65			66								
23.2	1	2-5	144	144	38868	22			1770								
Sum		2-5	718	716		113	6.35 ± 0.24	6.35 ± 0.24		(3.80 ± 0.14) x 10^{-3}	14.1	0.99	14.56	15.7	0.60	(2.10 ± 0.17) x 10^{-3}	180 ± 20
	1	0	1272	1266	3184	1											
	1	2,6	322	322	180870	110	2.92 ± 0.16	2.92 ± 0.16	1640	(1.70 ± 0.09) x 10^{-3}	14.99	1.09	15.5	16.7	0.57	(8.0 ± 1.2) x 10^{-4}	65 ± 10
23.7	1	2,4,6	138	138	148960	89	1.55 ± 0.13		1675	(0.90 ± 0.075) x 10^{-3}	16.03						

TABLE IX

EXPERIMENTAL DATA

P,* kw	Radiator No.	Absrs.	Counts A	Counts B	Counts C	t, min	Counts per Minute A	Counts per Minute B	Counts per Minute C	$C_p/P(t\rho)$,* protons / kw mg/cm^2	E_{pl}, Mev	ΔE_p, Mev	$E_{pl} + f\Delta E_p$, Mev	E_n, Mev	σ_s, barns	$\Delta[C_p/P(t\rho)]$, counts / kw min mg/cm^2	N(E), neutrons / Mev kw sec
25.5	1	0	1208	1216	2170	1	At 1.85 kv			Gas check, drift 30 volts							
25.5	1	0	1228	1226	2902	1	At 1.88 kv										
25.5	1	1-7	0	4	31572	23	0 ± 0.18		1370	Background check							
25.5	1	2,4,6	188	188	193032	149	1.26 ± 0.09		1295	$(6.8 \pm 0.5) \times 10^{-4}$	16.03	0.818	16.42	17.7	0.53	$(2.2 \pm 0.7) \times 10^{-4}$	26 ± 8
25.7	1	1-4,6	101	102	159054	118	0.86 ± 0.085		1350	$(4.6 \pm 0.46) \times 10^{-4}$	16.85	1.14	17.39	18.7	0.50	3.2 ± 0.6	28 ± 5
25.7	1	3,5,6	23	23	108044	90	0.26 ± 0.05		1200	$(1.4 \pm 0.3) \times 10^{-4}$	17.95	2.0	18.83	20.25	0.45	0.5 ± 0.3	2.8 ± 1.7
25.9	1	2,6,7									19.88						
25.9	1	0	1280	1286	2840	1	At 1.88 kv, gas OK										
25.9	1	2,6,7	22	22	140100	131	0.17 ± 0.035		1070	0.9 ± 0.2	19.88	1.96	20.8	22.4	0.40		
25.9	1	2,6,7	8	8	24034	43	0.18 ± 0.06		570		19.88						
Sum	1	2,6,7	30	30		174	0.17 ± 0.03			0.9 ± 0.16		1.96	20.8	22.4	0.40	0.5 ± 0.2	3 ± 1.5
0	1	2,6,7	0	0		60	< 0.02			Background run							
25.9	1	5-7	2	4	24872	40					21.78						
25.9	1	5-7	7	7	56052	100	0.070 ± 0.026			0.38 ± 0.14	21.78	1.7	22.55	24.3	0.36	0.22 ± 0.17	1.8 ± 1.3
25.9	1	1-7	2	2	37930	67	0.03 ± 0.02			0.16 ± 0.1	23.4						

*Heat balance power indication used. For all of these runs the automatic control indicated that the power was 20 kw. The discrepancy was not understood but the heat balance measurement is thought to be more reliable.

TABLE X

EXPERIMENTAL DATA

P, kw*	Radiator No.	Absrs	Counts A	Counts B	Counts C	t, min	Counts per Minute A	Counts per Minute B	Counts per Minute C	$C_p/P(t\rho)$,* protons / kw mg/cm²	E_{pl}, Mev	ΔE_p, Mev	$E_{pl} + f\Delta E_p$, Mev	E_n, Mev	σ_s, barns	$\Delta[C_p/P(t\rho)]$, counts / kw min mg/cm²	$N(E)$, neutrons / Mev kw sec
25.9	1	0	3504	13598	7682	3	1170	4530	2560								
25.9	1	0	2214	7884	4014	2	1108	3935	2007								
25.9	1	0	4946	16578	10476	4	1233	4140	2615								
25.9	3	0	7574	30864	30908	21	360.5 ± 4	1470 ± 8	1470	2.53 ± 0.03	6.30	0.62	6.60	7.1	1.25	1.148 ± 0.03	$(7.5 \pm 0.2) \times 10^4$
25.9	3	2	8492	31118	50706	41	270 ± 2	759 ± 4	1240	1.45 ± 0.014	6.87	1.26	7.45	8.0	1.14	0.99 ± 0.03	$(3.5 \pm 0.1) \times 10^4$
25.9	3	4	3046	8532	46194	44	66.2 ± 1.2	185 ± 2	1050	0.464 ± 0.008	8.19	1.05	8.69	9.3	0.92	0.262 ± 0.01	$(1.37 \pm 0.05) \times 10^4$
25.9	3	3,4	748	1788	21452	26	28.8 ± 1	68.7 ± 1.6	826	0.202 ± 0.007							
25.9	4	3	3200	9604	13694	11	291 ± 5	875 ± 9	1242	0.555 ± 0.01	7.92	0.64	8.23	8.85	1.05	0.232 ± 0.011	$(1.75 \pm 0.08) \times 10^4$
25.9	4	4	3724	9988	27562	22	169 ± 2.8	454 ± 4.5	1250	0.322 ± 0.005	8.53	1.05	9.02	9.70	0.96	0.172 ± 0.007	$(8.6 \pm 0.35) \times 10^3$
25.9	4	3,4	1020	2260	14882	13	78 ± 2.5	174 ± 4	1140	0.150 ± 0.005	9.57	1.87	10.41	11.20	0.85	0.11 ± 0.005	$(3.6 \pm 0.3) \times 10^3$
1.95	4	2,5	338	586	32430	18	18.8 ± 1	32.6 ± 1.3	1800	$(3.58 \pm 0.2) \times 10^{-2}$	11.40	1.10	11.92	12.83	0.75	$2.26 \pm 0.26 \times 10^{-2}$	$(1.4 \pm 0.16) \times 10^3$
1.90	4	1,4,5	496	838	77946	72	6.9 ± 0.3	11.6 ± 0.4	1080	$(1.31 \pm 0.06) \times 10^{-2}$	12.45	0.97	12.90	13.88	0.69	$6.8 \pm 0.6 \times 10^{-3}$	$(5.1 \pm 0.4) \times 10^2$
1.90	4	2-5	296	474	92078	89	3.3 ± 0.2	5.3 ± 0.2	1030	$(6.3 \pm 0.4) \times 10^{-3}$	13.43	0.99	13.89	14.93	0.64	$3.4 \pm 0.45 \times 10^{-3}$	$(2.7 \pm 0.3) \times 10^2$
1.90	4	2,6								$(2.9 \pm 0.2) \times 10^{-3}$	14.36	1.09	14.87	16.0	0.60		
1.90	4	2,4,6									15.41						

*Heat balance power indication used. For all of these runs the automatic control indicated that the power was 25 kw. The discrepancy was not understood but the heat balance measurement is thought to be more reliable.

TABLE XI

EXPERIMENTAL DATA

P,* kw	Radiator No.	Absrs.	Counts per Minute	$C_p/P(t\rho)$, protons / kw mg/cm^2	$E_p + f\Delta E_p$, Mev	E_n, Mev	σ_s, barns	ΔE_p, Mev	$N(E)$, neutrons / Mev kw sec
25.9	3	0	1470 ± 8	10.3 ± 0.056	5.39	5.80	1.45	1.70	(2.11 ± 0.01) x 10^5
25.9	3	2	759 ± 4	5.32 ± 0.028	6.10	6.55	1.32	1.58	(1.29 ± 0.007) x 10^5
25.9	3	4	185 ± 2	1.29 ± 0.014	7.48	8.05	1.13	1.34	(4.32 ± 0.047) x 10^4
25.9	3	3,4	68.7 ± 1.6	0.48 ± 0.011	8.58	9.24	1.02	1.21	(1.97 ± 0.045) x 10^4
25.9	4	3	875 ± 9	1.67 ± 0.017	7.18	7.72	1.22	1.39	(5.00 ± 0.05) x 10^4
25.9	4	4	454 ± 4.5	0.865 ± 0.0086	7.90	8.50	1.18	1.29	(2.88 ± 0.03) x 10^4
25.9	4	3,4	174 ± 4	0.332 ± 0.0076	8.94	9.61	1.00	1.17	(1.43 ± 0.03) x 10^4
25.9	4	2,5	32.6 ± 1.3	0.062 ± 0.0025	10.87	11.70	0.81	1.01	(3.83 ± 0.15) x 10^3
25.9	4	1,4,5	11.6 ± 0.4	0.022 ± 0.00076	11.95	12.85	0.77	0.93	(1.56 ± 0.05) x 10^3
25.9	4	2-5	5.3 ± 0.25	0.01 ± 0.0005	12.94	13.92	0.69	0.88	(8.4 ± 0.41) x 10^2

*Heat balance power indication used. For all of these runs the automatic control indicated that the power was 25 kw. The discrepancy was not understood but the heat balance measurement is thought to be more reliable.

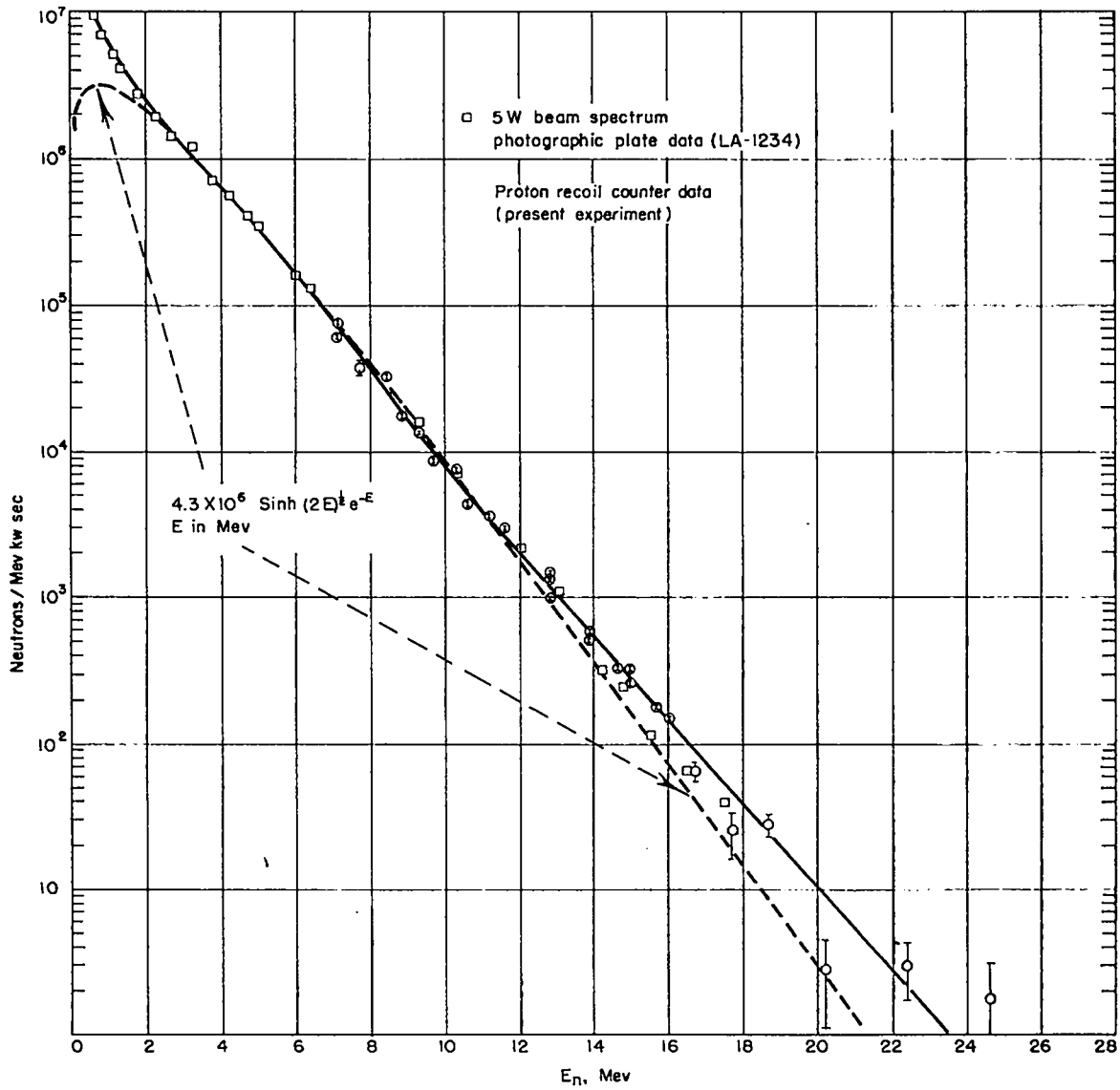

Fig. 5 - Composite plot of beam spectrum.

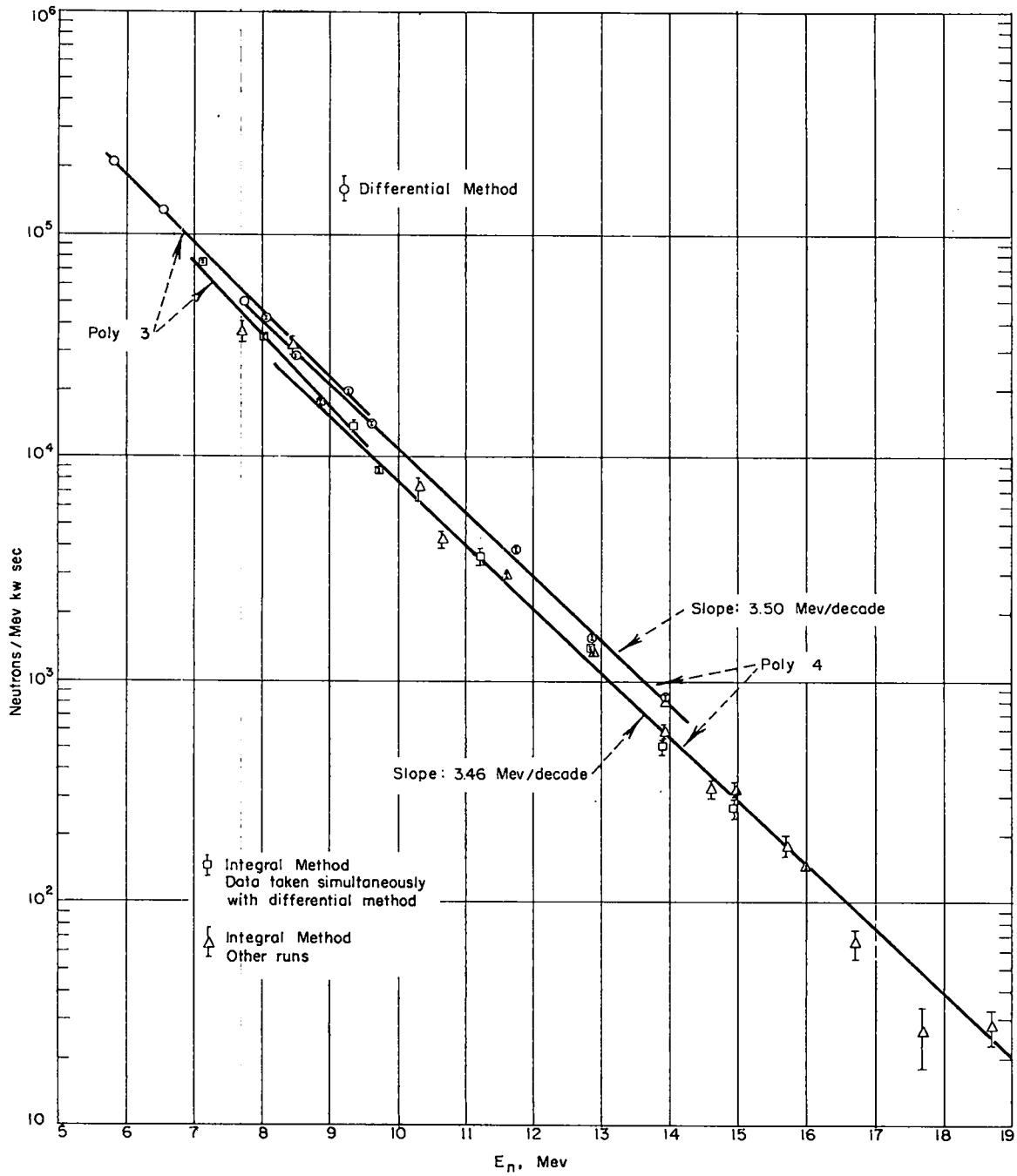

Fig. 6 - Comparison of the neutron spectra observed with differential and integral proton counting. Note that the slopes are the same. The difference in absolute values results from poor proton counting efficiency, giving an error in absolute values but not in shape.

The appearance of 25 Mev neutrons seems to imply that a reasonably large fraction of the fission fragments are formed with at least 30 Mev excitation, considerably above the 20 Mev average derived from the liquid-drop model and roughly checked by experimental indications.

If the range of total fragment kinetic energy observed by Brunton and Hanna [Canadian Journal of Research 28A, 190 (1950)] for particular mass ratios can be interpreted as the range of excitation energy in the fragments, it is easy to believe that excitations larger than 40 Mev can exist with fair probability.